INFLUENCE OF COMPUTED TOMOGRAPHY PARAMETERS ON THE RADIOTHERAPY PLAN CALCULATION

Enis Tinjak
Radiotherapy department, Clinical Center of Sarajevo University, Bosnia and Herzegovina,
enis.tinjak@fzs.unsa.ba
Adnan Beganovic
Radiology Clinic, Clinical Center of Sarajevo University, Bosnia and Herzegovina.
adnanbeg@gmail.com
Velda Smajlbegovic
Radiotherapy department, Clinical Center of Sarajevo University, Bosnia and Herzegovina.
veldasmajl@hotmail.com
Fuad Julardzija
Department for Radiology Technology, Faculty of Health Studies, University of Sarajevo, Bosnia and Herzegovina, fuad.julardzija@fzs.unsa.ba
Adnan Sehic
Radiotherapy department, Clinical Center of Sarajevo University, Bosnia and Herzegovina,
adnan.sehic@fzs.unsa.ba
Sabina Prevljak
Radiology Clinic, Clinical Center of Sarajevo University, Bosnia and Herzegovina,
sabinarad@yahoo.com
Branka Metlic
Radiotherapy department, Clinical Center of Sarajevo University, Bosnia and Herzegovina,
brankametlic@gmail.com
Nusret Salkica
Clinic for Nuclear Medicine, Clinical Center of Sarajevo University, Bosnia and Herzegovina,
nusret_nt@hotmail.com
Muhamed Topcagic
Clinic for Oncology and Radiotherapy, Department for Radiotherapy, University Clinical Center Tuzla, Bosnia and Herzegovina, muhamed.rt@hotmail.com

Abstract: Contouring, planning and dose calculation in treatment planning systems (TPS) are based on computed tomography (CT) images. Therefore, it is important to have developed, optimized and adapted scanning protocols for specific anatomic regions and special radiotherapy modalities such as stereotactic radiosurgery (SRS). The aim of this study was to determine influence of tube voltage, field of view size (FOV) and reconstruction kernels on CT numbers and the resulting radiotherapy (RT) dose calculation.

This study was performed at Clinic of Oncology, Clinical Center University of Sarajevo. Verification electron density and CT number values was performed using CIRS Thorax 002LFC phantom, while anthropomorphic CIRS 038 phantom for stereotactic end-to-end verification was used for the purpose of dose plan calculation analysis with large bore CT simulator Canon Aquillion LB.The significant correlation between the tube voltage and the measured values of CT numbers is significant for all materials ($p < 0.05$), except for water ($p = 0.310$). No significant correlation between FOV and obtained values of CT numbers was found in any of the evaluated tissue equivalent materials. Evaluating the impact of reconstruction kernels on Hounsfield units (HU), significant deviations were found for the FC62, FC68 and FC07 reconstruction kernels. Also, analyzing the influence of reconstruction kernels on the RT dose calculation, the extreme values are associated with D_{min}/D in PTV for kernels FC41 and FC68, where deviations from the values obtained using the baseline scanning parameters were -1.3% and -1.9%. For deviation of 1 HU in muscle tissue of CIRS 002LFC, the calculated D_{min}/D in PTV of CIRS STEEV phantom will reduce by 0.79%. Similarly, the reduction of D_{98} and D_2 would be 6.8 cGy and 3.03 cGy for 1 HU, respectively. Change of the reconstruction kernels caused differences of 0.4% in D_{min}/D calculation in clinical target volume (CTV).

CT scanning and reconstruction parameters may affect Hounsfield units, which could have an impact on dose calculations in RT plan. Hence, it is recommended to standardize the scanning protocol used in calibration curve generation for TPS. One should avoid use of different tube voltages and kernels, while according to this study, the change of FOV will have no impact on dose calculations.

Keywords: Hounsfield unit, CT protocols, dose calculation, radiotherapy, SRS plan.

1. INTRODUCTION

Computed tomography (CT) is a radiological procedure in which a narrow x-ray beam is directed at a patient, generating signals that the computer processes to produce cross-sectional images. With the improvement of CT it is possible to distinguish densities that differ by only 0.2%, using a large number of very sensitive detectors in the CT device (Čatić Dž, Bešlić Š, Smajlović F, Hadžihasanović B, 2007). In radiotherapy (RT), CT is used for RT treatment planning. CT image stack serves a dual role in radiotherapy treatment planning. On one hand, it provides anatomical information used by the radiation oncologists for delineation of the target and the organs at risk. On the other hand, it provides a 3D distribution of electrons, which is used in dose calculation. To achieve both roles, imaging parameters need to be optimized and then used consistently. In this regard, high quality CT image is essential for accurate delineation and RT treatment planning (Chen et al., 2017). The purpose of CT simulation in RT is to provide quantitative segmentation of the target volume and healthy structures at risk, which plays a key role in accurate planning of RT treatment. Accurate segmentation relies on visibility of the tumor and healthy normal structures on CT images, interpretation of radiologic anatomy and understanding of potential tumor involvement areas based on tumor biology (Li et al., 2014; Mileusnić D, et al., 2020).

The American Medical Physicists Association (AAPM) recommends that CT scanning protocols should be developed, optimized and adapted to specific treatment sites and anatomic regions (Mutic et al., 2003). The process of optimization requires that the scan protocol parameters are adjusted to ensure high image quality while achieving an appropriate clinically acceptable radiation dose (Verdun et al., 2015). The CT device determines the location and radiodensity of the patient's organs in specific coordinates, pixels. Each pixel is represented by a CT number expressed in terms of Hounsfield units (HU), which describes the amount of radiation attenuation in a patient's organ. The electron density of the organ tissue is expressed in terms of relative electron density (RED). The relationship between the RED and the CT numbers must be determined and imported to the TPS. Among other things, the TPS will based its dose calculation on the calibration curve RED = f (HU) (Afifi et al., 2020). The calibration curve is a function of HU versus RED for a range of materials with different densities represented as a table. If there is a discrepancy between the HU values on the CT image for specific tissue types and the HU values in the TPS calibration curve, errors would be introduced in the TPS calculation. Thus, any inaccuracy in the CT number will have an impact on the dose calculated by TPS (Cozzi et al., 1998; Kolarevic et al., 2020). The tube voltage (kV) is the most important parameter affecting the calibration curve. The RT dose calculated from images acquired at different tube voltages can be within ±2% (Guan et al., 2002). The aim of this study is to determine the effect of tube voltage, field of view size, and the choice of reconstruction kernels on the HU values and the resulting RT dose calculation.

2. MATERIAL AND METHODS

The research was conducted as a dosimetric experimental study in the Clinic of Oncology, Clinical Center University of Sarajevo. Aquillion LB (Canon Medical Systems, Japan) CT simulator was used to acquire images. Phantom thorax model 002LFC (CIRS, Norfolk, USA) was used to analyze the effects of scanning and reconstruction parameters on the CT number (HU). The phantom contains cylindrical inserts of known RED, which simulate the attenuation characteristics equivalent to water, muscle, fat, bone, and lung, as well as the location where a syringe of any content can be inserted (in our case distilled water). The phantom was scanned in helical mode by changing scanning parameters such as tube voltage (U), field of view size (FOV) and reconstruction algorithms (kernels). A series of CT images was obtained by changing the tube voltage in steps of 80 kV, 100 kV, 120 kV and 135 kV, changing the FOV from 240 mm (S), 320 mm (M), 400 mm (L), 550 mm (LL) to 700 mm (XL) diameter, and changing various kernels. CT numbers were measured in different regions of interest (ROI). The kernel, also known as a convolution algorithm, refers to the process used to modify the frequency contents of projection data prior to back projection during image reconstruction in a CT scanner. Different kernels have been developed for specific anatomical applications including soft tissue and bone. We analyzed HU values by changing the following reconstruction algorithms: head algorithms with beam hardening correction (BHC) fine grain size (FC20, FC25, FC26), head algorithms with BHC coarse grain size (FC62, FC68) head algorithms without BHC (FC41, FC46, FC47, FC49), body algorithms without BHC (FC07, FC11, FC15, FC18-H, FC18), bone algorithms for sharp images (FC30, FC35) and high resolution lung algorithm (FC56). All algorithms are based on manufacturer's iterative reconstruction technique called Three-Dimensional Adaptive Iterative Dose Reduction (AIDR 3D).

In the second part of the study, the anthropomorphic phantom for stereotactic radiosurgery and radiotherapy (SRS/SRT) end-to-end verification, STEEV 038 (CIRS, Norfolk, USA), was scanned to be used for SRS plan. The scanning and reconstruction parameters matched those used for imaging of 002LFC thorax phantom. Contouring of target volumes was done by a radiation oncologist. Clinical target volume (CTV) and planning target volume (PTV) were position in the central part of brain tissue equivalent. The plan included contours of the various organs at risk

(OAR). The isocenter was placed in the middle of the PTV. The reference CT images were obtained using scan parameters identical to those used for defining the calibration curve (120 kV and 550 mm FOV). Based on the reference CT images, a reference radiation plan for SRS was created in TPS using 6 MV photon energy and Volumetric Modulated Arc Therapy (VMAT) irradiation technique. This was a baseline plan used for further dose calculations. Registration of the newly acquired image was performed by automatically overlapping the images in 6 degrees of freedom (6 DoF). The base plan in TPS was copied to the new sets of images obtained by changing various scanning and reconstruction parameters. Dose calculations were repeated for each set of images. The relative values of the minimum (D_{min}), mean (D_{mean}), and maximum (D_{max}) doses with respect to the prescribed dose (D) were selected as basic predictors of the RT plan calculation. Also, the analysis of the dose value close to the minimum (D_{98}) and dose value close to maximum (D_2) in the PTV, was performed for different field of view size (FOV) and tube voltages. To analyze influence of reconstruction kernels to artifacts, CT numbers were measured in two regions of interest (ROI) of the STEEV phantom that were localized in the brain tissue – the first one near bone structures (10 mm) and another one at a significant distance (40 mm) corresponding to the center of the brain tissue. Phantom was scanned using fixed tube voltage (120 kV), constant tube loading (370 mAs) and FOV (550 mm). Review and analysis of RT plans were performed using dose-volume histograms (DVH) and dose statistics in the Eclipse ver. 15.5 TPS (Varian Medical Systems, Palo Alto, USA). In total, 28 dose calculations were performed using different image sets for the SRS plan.

The SPSS 26.0 statistical data analysis program (IBM Corporation, Armonk, USA) was used for the database and data processing. Descriptive statistics methods were used to analyze numerical data. Student's t-test was used for comparison of variables whose distribution is normal. The Kruskal–Wallis test or one-way ANOVA on ranks was used for testing whether non-parametric samples originate from the same distribution. Correlations between variables were examined using Pearson's correlation test. A significance level of $\alpha = 0.05$, was used.

3. RESULTS

Evaluation of scanning and reconstruction parameters on Hounsfield units

In the first part of the study, the CT numbers were evaluated under the influence of different tube voltages and FOV. No significant correlation between FOV and obtained values of CT numbers was found in any of the evaluated tissue equivalent materials (Table 1). On the other hand, the correlation between the tube voltage and the measured values of CT numbers is significant for all materials, except for water (Table 1). If the CT is properly calibrated on all tube voltages the value of the CT number of water should be equal to zero (0 HU), or inside the tolerance levels for RT (±5 HU).

Table 1. CT numbers for different tissue equivalent materials (HU) that correspond to different tissue equivalent materials in CIRS phantom for different field of view (FOV) and tube voltage (kV) values. Correlation coefficients (r) and significance values (p) of correlation test between field of view (FOV) and tube voltage (kV) with CT numbers are presented in bottom rows.

		CT numbers for different tissue equivalent materials (HU)							
Field of View	Tube voltage (kV)	Water equivalent	Muscle	Water	Adipose tissue	Bone core	Air	Bone	Lungs
S	80	-2.7	52.8	-0.5	-89	1250.7	-1002.4	1264.1	-810.8
	100	-5	50.8	-0.3	-77.9	992.7	-1001.2	1011.3	-808.8
	120	-6.7	50.5	0.8	-71.3	843.8	-1000.3	868	-807.6
	135	-7.8	49.4	0.4	-68.5	762.4	-1001.4	783.6	-808
M	80	-3.2	52.5	0.9	-90.4	1251.3	-1002.4	1264.5	-811.5
	100	-5	51.3	-0.1	-77.9	997.8	-1000.3	1011.9	-808.8
	120	-6.3	50.4	-0.2	-70.6	851	-1000.3	867.6	-807.6
	135	-7.9	48.9	-0.8	-68	763.1	-1000.6	783.2	-807.8
L	80	-1.9	53.7	0.6	-91.9	1237.9	-1000.5	1268.7	-810.4
	100	-4.5	51.5	1.6	-79.7	981.8	-999.5	1012.8	-808.2
	120	-5.3	50.9	0.8	-71.7	849.9	-998.6	870.1	-807.3
	135	-7	49.1	-1.6	-70	786	-999.5	785.5	-807.6
LL	80	-4.1	51.6	-0.5	-91.8	1271.1	-1001.8	1293.3	-812.4
	100	-5.9	49.9	0.0	-79.5	1027.4	-1000	1017.8	-810
	120	-7.9	49.4	3.2	-71.8	887.6	-999.9	861.3	-808.9
	135	-8	48.7	2.5	-68.9	786.4	-999.7	767.5	-809
XL	80	-4	50.5	-3.5	-92.8	1237.1	-1002.3	1265.9	-811.8
	100	-6.1	49	1.6	-80.2	1003.1	-999.8	1010.7	-810
	120	-6.4	49.4	1.2	-72.5	886.4	-1000.7	869.2	-809.1
	135	-8.2	47.8	0.0	-70	811.5	-1000.1	784.6	-808.4
FOV	*r*	-0.178	-0.386	0.058	-0.215	0.129	0.294	0.055	-0.362
	p	0.453	0.093	0.807	0.364	0.588	0.208	0.817	0.117
kV	*r*	-0.931	-0.814	-0.303	0.969	-0.969	0.496	-0.969	0.745
	p	<0.001	<0.001	0.193	<0.001	<0.001	0.026	<0.001	<0.001

To evaluate influence of the reconstruction algorithms on the mean CT numbers, the following kernels were switched: FC07, FC11, FC15, FC18-H, FC18, FC20, FC25, FC26, FC30, FC35, FC46, FC47, FC49, FC41, FC56, FC62, and FC68. The results showed that reconstruction kernels FC62, FC68, and FC07, had extreme values stand out that deviate significantly from the rest of the data. For the FC62 kernel, the materials that corresponds to water and muscle, deviate from the mean by 3.97 HU and 16.91 HU, respectively. For materials simulating muscle and adipose tissue, the mean values deviations for the FC68 kernel, are 10.91 HU and -6.41 HU, respectively. When the FC07 reconstruction kernel is used, the material simulating bone had a 75.74 HU higher HU, results shown in the figure (
Figure ***1***).

Figure 1. Deviations of the measured CT number for each reconstruction kernel in relation to the mean value of the CT number for different phantom materials. Extreme values marked with circles and asterisks are shown.

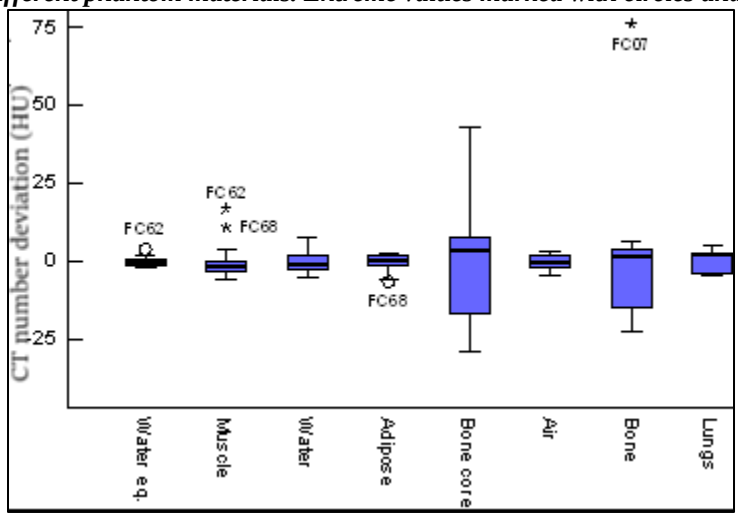

To evaluate the effect of reconstruction kernels on the presence of artefacts, we measured CT numbers in ROIs near and away from the bone structures of the skull. The results show that significant difference in the value of CT numbers between two ROIs exists for most evaluated kernels. The *p*-value was calculated using Student's *t* test for paired samples, using measurement results from the same tissue. For two out of nine analyzed kernels (FC25 and FC49), this difference was not significant. When using these kernels, the artifacts could not be visualized on the image, as no significant differences in the CT numbers between 2 regions of interest exist (**Error! Reference source not found.**

Table 2. Mean value ($\bar{x}$) and standard deviation (σ) of the measured CT number in the STEEV phantom near and away from the bone structures of the skull in the brain tissue region, the difference Δx and the result of t test and associating p-value.

Kernel	Near the bone		Away from the bone		Difference		
	$\bar{x}$	σ	$\bar{x}$	σ	Δx	*t*	*p*
FC18	66,2	10,3	52,8	7,4	13,4	33.4	<0,001
FC25	40,7	12	41,1	10,1	-0,4	0.807	0,420
FC35	65,1	33,6	53,9	29	11,2	7.98	<0,001
FC46	65,4	10	53,4	7	12	31.1	<0,001
FC56	64,5	21,1	53,8	17,7	10,7	12.3	<0,001
FC62	41,9	5,8	43,1	4,3	-1,2	5.26	<0,001
FC68	40,3	9,9	43,2	7,7	-2,9	7.31	<0,001
FC41	64,4	7,6	52,9	5,4	11,5	39.0	<0,001
FC49	42	11	42,2	9,1	-0,2	0.443	0.658

Evaluation of radiotherapy plans

The phantom CIRS STEEV was used to evaluate SRS radiotherapy planning. CTV, PTV and contours of OAR were delineated. The relative values of the maximum, mean, and minimum doses (D_{max}, D_{mean}, and D_{min}) in relation to the

prescribed dose (D), the value of which is usually expressed as a percentage, were chosen as the basic indicators for calculating the radiotherapy plan.

Table 3 shows values of the minimum, mean and maximum dose in relation to the prescribed dose (D_{min}/D, D_{mean}/D and D_{max}/D) in the PTV, near minimum (D_{98}) and near maximum (D_2) in PTV, as well as corresponding deviation from the reference values for different FOV and tube voltages. Results of Kruskal-Wallis tests presented in the table indicate that no significant differences between dosimetric values can be found amongst different FOV. However, these differences are significant in the case of different tube voltages.

In stereotactic radiotherapy, one of the most important indicators of the quality of the radiotherapy plan is D_{min}/D, in the PTV, its value should not be lower than 95%. No part of the PTV should receive a dose less than 95% of the prescribed. This is the case for 20 plans listed in the Table 3.

Table 3. Analysis of the value of the minimum, mean and maximum dose in relation to the prescribed dose (D_{min}/D, D_{mean}/D and D_{max}/D) in planning target volume (PTV), and corresponding deviation from the reference value ($\Delta D_{min}/D$, $\Delta D_{mean}/D$ and $\Delta D_{max}/D$), near minimum (D_{98}) and near maximum (D_2) and corresponding deviation from the reference value (ΔD_{98} and ΔD_2) in PTV for different field of view (FOV) and tube voltage (U) in STEEV phantom. Results of Kruskal-Wallis tests are presented in bottom rows for FOV and U as grouping variables.

FOV	U (kV)	D_{min}/D (%)	$\Delta D_{min}/D$ (%)	D_{mean}/D (%)	$\Delta D_{mean}/D$ (%)	D_{max}/D (%)	$\Delta D_{max}/D$ (%)	D_{98}	ΔD_{98}	D_2	ΔD_2
S	80	93.2	-2.9	112.3	-0.3	122.6	-0.6	1837	-6	2152	-8
	100	94.8	-1.3	112.4	-0.2	122.7	-0.5	1846	3	2156	-4
	120	94.5	-1.6	112.5	-0.1	122.7	-0.5	1821	-22	2160	0
	135	97.2	1.1	112.6	0.0	122.7	-0.5	1861	18	2168	8
M	80	94.6	-1.5	112.8	0.2	122.7	-0.5	1841	-2	2153	-7
	100	95.8	-0.3	112.6	0.0	122.9	-0.3	1849	6	2157	-3
	120	94.9	-1.2	112.7	0.1	122.9	-0.3	1826	-17	2160	0
	135	97.4	1.3	112.8	0.2	122.9	-0.3	1861	18	2168	8
L	80	95.6	-0.5	112.8	0.2	122.9	-0.3	1846	3	2153	-7
	100	96.1	0	113.1	0.5	122.9	-0.3	1853	10	2157	-3
	120	94	-2.1	112.4	-0.2	123.2	0.0	1832	-11	2160	0
	135	97.8	1.7	112.9	0.3	123.2	0.0	1867	24	2168	8
LL	80	96.1	0	112.5	-0.1	123.2	0.0	1851	8	2154	-6
	100	96	-0.1	112.6	0.0	123.2	0.0	1856	13	2159	-1
	120*	96.1	0	112.7	0.1	123.2	0.0	1843	0	2160	0
	135	97.7	1.6	113.4	0.8	123.4	0.2	1868	25	2168	8
XL	80	96.3	0.2	113.4	0.8	123.4	0.2	1861	18	2155	-5
	100	96.6	0.5	113.4	0.8	123.5	0.3	1869	26	2160	0
	120	96.1	0	113.5	0.9	123.5	0.3	1839	-4	2161	1
	135	100.7	4.6	113.8	1.2	123.4	0.2	1903	60	2167	7
FOV	*H*	5.401		3.226		0.130		4.857		0.618	
	p	0.249		0.521		0.998		0.302		0.961	
U	*H*	11.45		13.24		18.63		13.23		17.87	
	p	0.010		0.004		<0.001		0.004		<0.001	

*Reference value

Dependence of D_{min}/D, D_{mean}/D and D_{max}/D in PTV, as well as D_{98} and D_2, on CT number values (HU) was examined for different tissue equivalent materials in CIRS LFC002 phantom. Correlation coefficients (r) and significance values (p) of correlation test are presented in **Error! Reference source not found.**. The most prominent results were associated with muscle tissue, where correlation of CT numbers with all dosimetric quantities was significant (Table 4).

Table 4. Correlation coefficients (r) and significance values (p) of correlation test between minimum dose (D_{min}), mean dose (D_{mean}) and maximum dose (D_{max}) in relation to the prescribed dose (D), near minimum (D_{98}) and near maximum dose (D_2) in planning target volume (PTV), and CT numbers in different tissue equivalent materials.

		Water equivalent	Muscle	Water	Adipose tissue	Bone core	Air	Bone	Lung
D_{min}/D (%)	*r*	-.623	-.731	-.035	.395	-.454	.265	-.484	.179
	p	.003	.000	.884	.085	.045	.258	.031	.450
D_{mean}/D (%)	*r*	-.620	-.802	-.257	.481	-.551	.357	-.555	.163
	p	.004	.001	.273	.032	.012	.123	.011	.493
D_{max}/D (%)	*r*	-.922	-.813	-.285	.948	-.956	.541	-.952	.728
	p	.001	.001	.223	.001	.001	.014	.001	.001
PTV D_{98} (cGy)	*r*	-.379	-.575	-.148	.132	-.194	.116	-.225	-.047
	p	.099	.008	.534	.580	.413	.625	.340	.845
PTV D_2 (cGy)	*r*	-.899	-.855	.118	.868	-.904	.518	-.910	.680
	p	.000	.000	.619	.000	.000	.019	.000	.001

Figure ***2*** provides information regarding dependence of D_{min}/D, D_{98} and D_2 in PTV on CT number values (HU) in muscle tissue as measured in CIRS 002LFC phantom for the corresponding imaging technique. The figures show linear regression curves. The parameter *b* represents the slope of the curve and has values of -0.79 %/HU, -6.8 cGy/HU and -3.03 cGy/HU. Thus, we can say that for deviation of 1 HU in muscle tissue of CIRS 002LFC, the calculated D_{min}/D in PTV of CIRS STEEV phantom will reduce by 0.79%. Similarly, the reduction of D_{98} and D_2 would be 6.8 cGy and 3.03 cGy for 1 HU, respectively.

Figure 2. Dependence of the relative value of the minimum dose (D_{min}) in relation to the prescribed dose (D) and near minimum dose (D_{98}) on the value of CT number of materials equivalent to muscle tissue for the PTV. Figures show linear regression curves (solid line, y = a + bx) and 95% mean confidence interval (dashed line) with parameters: (a) a = 135.7 ± 8.7; b = -0.79 ± 0.17, (b) a = 2199 ± 117; b = -6.8 ± 2.3 and (c) a = 2313 ± 22; b = -3.03 ± 0.44.

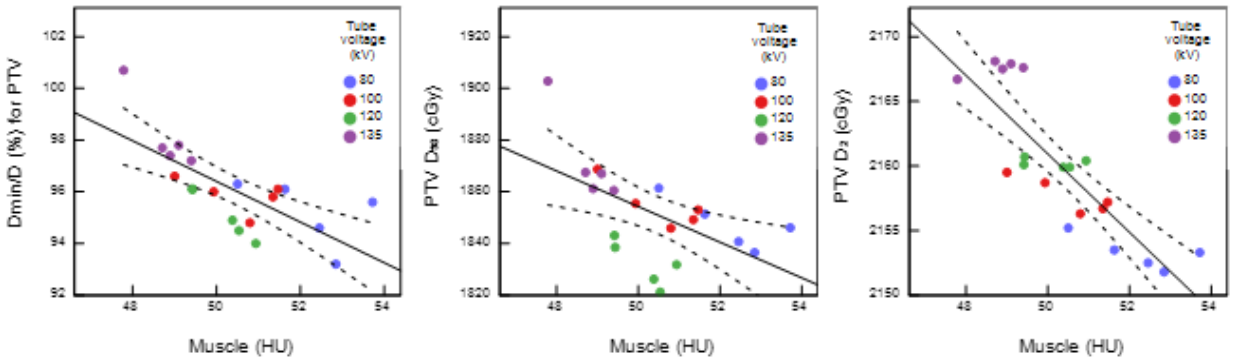

The study analyzed the influence of reconstruction kernels for head (FC25, FC35, FC41, FC46, FC49, FC56, FC62 and FC68) on the RT dose calculation. Analysis of minimum, mean and maximum dose values (D_{min}, D_{mean} and D_{max}) in relation to the prescribed dose (D) for different reconstruction kernels in CTV and PTV and differences in relation to the reference value (Δ) when using the FC25 kernel. The extreme values are associated with D_{min}/D in PTV for kernels FC41 and FC68, where deviations from the values obtained using the baseline scanning parameters (FC25) were -1.3% and -1.9%.

4. DISCUSSION

Variations in tube voltage values and selection of reconstruction kernels have a significant impact on the quality of the CT image and on the dose calculation of the radiotherapy plan.

The main predictor for the differences in the HU is the tube voltage, which is described in the analysis of the results obtained by scanning the phantom "CIRS 002LFC". At higher tube voltage, the X-rays are more penetrating, and therefore the material looks more radio-transparent to them, which yields lower HU values for muscle, bone and bone core. The results showed that 135 kV leads to lower HU, and 80 kV to higher HU values (Table 1), which is in accordance with results published by Zheng X et al. who analyzed CT numbers in the center of two phantoms of different sizes. In their study the largest difference in CT number (174 HU) was observed for tissue equivalent material “Bone1250” under tube voltage of 80 keV (Zheng et al., 2020).

Figure ***1*** illustrates how different kernels affect Hounsfield units in different tissue equivalent materials. Extreme values are associated with FC62 and FC68, both commonly used for head imaging with BHC and coarse grain size, and body algorithm FC07. Our results are corroborated by study Davis AT et al. indicating that the values of HU are most affected by variations in the reconstruction algorithm where the maximum variation of HU in the range of selected algorithms was up to 117 HU (±59 HU) for a RED of 2.00, representing bone-like material. For material with RED equal to 0.998, which is close to water, the maximum measured variation of HU was 56 HU (±28 HU). However, it should be noted that reconstruction algorithms in the same group of body regions have a smaller deviation from HU compared to each other. For example, FC42 provides similar HU values as FC44 and FC13 compared to FC15 which is in accordance with (Davis et al., 2018).

Results in our study show that dosimetric quantities D_{min}/D (%),D_{mean}/D and D_{max}/D in the PTV, as well as D_{98} and D_2, are affected by the tube voltage, while dependence on FOV had not been found significant (Table 3). While these results were based on calcuations in STEEV phantom, they could be linked back to CT number measurements made on 002LFC phantom imaged with same scan and reconstruction parameters. As mentioned earlier, tube voltage affected CT numbers as well, so we evluated the same correlations could be drawn between change of CT numbers and selected dosimetric quantities. Indeed, the significant correlation had been observed for many of the evaluated tissues (Table 4**Error! Reference source not found.**). The most prominent example is the muscle equivalent tissue, whose CT numbers correlate with all three evaluated dosimetric quantities in PTV – D_{min}/D (%), D_{98} and D_2 (

Figure ***2***).

It is not expected for such small differences in Hounsfield units to have an impact on the mean dose delivered to PTV by a 6 MV linear accelerator. However, small deviations in CT numbers inside or outside of PTV could affect the D_{min}/D (%), D_{98} and D_2. These values could go outside of recommended limits (i.e. <95% of D_{min}/D in PTV). Hence, the plan would be subjected to changes during the optimization process. This, in turn, can lead to overexposure of OAR or underexposure of PTV. When evaluating the influence of the reconstruction kernels on the dose calculations, the extreme values were associated with D_{min}/D in PTV for kernels FC41 and FC68. FC68 is one of the kernels that affected CT numbers in 002LFC phantom (

Figure ***1***). Interestingly, this kernel is commonly used for head imaging, and therefore could be utilized in SRS for brain tumors. The careful selection of kernels is of utmost importance as they could lead to different dose calculations. Similar results were presented in a study by Davis AT et al, who indicated that for each image compared with the baseline image, the maximum change in HU for air, bone, and soft tissue was the maximum dose change to PTV or OAR. The magnitude of the HU change was largely dependent on the chosen reconstruction kernel. The difference in HU, resulting from a change in reconstruction kernel, is significantly greater than quality control tolerances in some cases (soft tissue, air). Changes in soft tissue HU had the greatest impact when the change in PTV dose was largest (above ± 0.5%) and exceeded a tolerance of ± 20 HU (Davis et al., 2019; Internationale Atomenergie-Organisation, 2004).

5. CONCLUSION

CT scanning and reconstruction parameters may affect Hounsfield units, which could have an impact on dose calculations in RT plan. Hence, it is recommended to standardize the scanning protocol used in calibration curve generation for TPS. One should avoid use of different tube voltages and kernels, while according to this study, the change of FOV will have no impact on dose calculations.

REFERENCES

Afifi, M. B., Abdelrazek, A., Deiab, N. A., Abd El-Hafez, A. I., & El-Farrash, A. H. (2020). The effects of CT x-ray tube voltage and current variations on the relative electron density (RED) and CT number conversion curves. *Journal of Radiation Research and Applied Sciences*, *13*(1), 1–11. https://doi.org/10.1080/16878507.2019.1693176

Čatić, Dž., Bešlić, Š., Smajlović, F., & Hadžihasanović, B. (2007). *Digitalne radiološke metode*. Visoka zdravstvena škola Univerziteta u Sarajevu.

Chen, G.-P., Noid, G., Tai, A., Liu, F., Lawton, C., Erickson, B., & Li, X. A. (2017). Improving CT quality with optimized image parameters for radiation treatment planning and delivery guidance. *Physics and Imaging in Radiation Oncology*, *4*, 6–11. https://doi.org/10.1016/j.phro.2017.10.003

Cozzi, L., Fogliata, A., Buffa, F., & Bieri, S. (1998). Dosimetric impact of computed tomography calibration on a commercial treatment planning system for external radiation therapy. *Radiotherapy and Oncology*, *48*(3), 335–338. https://doi.org/10.1016/S0167-8140(98)00072-3

Davis, A. T., Muscat, S., Palmer, A. L., Buckle, D., Earley, J., Williams, M. G. J., & Nisbet, A. (2019). Radiation dosimetry changes in radiotherapy treatment plans for adult patients arising from the selection of the CT image reconstruction kernel. *BJR|Open*, *1*(1), 20190023. https://doi.org/10.1259/bjro.20190023

Davis, A. T., Palmer, A. L., Pani, S., & Nisbet, A. (2018). Assessment of the variation in CT scanner performance (image quality and Hounsfield units) with scan parameters, for image optimisation in radiotherapy treatment planning. *Physica Medica*, *45*, 59–64. https://doi.org/10.1016/j.ejmp.2017.11.036

Guan, H., Yin, F.-F., & Kim, J. H. (2002). Accuracy of inhomogeneity correction in photon radiotherapy from CT scans with different settings. *Physics in Medicine and Biology*, *47*(17), N223–N231. https://doi.org/10.1088/0031-9155/47/17/402

Internationale Atomenergie-Organisation (Ed.). (2004). *Commissioning and quality assurance of computerized planning systems for radiation treatment of cancer*. International Atomic Energy Agency.

Kolarevic, G., Jaroš, D., Pavičar, B., Ignjć, T., Kostovski, A., Marosevic, G., Predojević, B., & Mirjanić, D. (2020). Computed tomography simulator conversion curve dependence on scan parameters and phantom dimension. *Journal of Health Sciences*. https://doi.org/10.17532/jhsci.2020.1085

Li, H., Yu, L., Anastasio, M. A., Chen, H.-C., Tan, J., Gay, H., Michalski, J. M., Low, D. A., & Mutic, S. (2014). Automatic CT simulation optimization for radiation therapy: A general strategy: CT simulation optimization for radiation therapy. *Medical Physics*, *41*(3), 031913. https://doi.org/10.1118/1.4866377

Mileusnić D, Marošević G, & Durbaba M,. (2020). *Radijaciona onkologija*. Medicinski fakultet Univerziteta u Banjoj Luci.

Mutic, S., Palta, J. R., Butker, E. K., Das, I. J., Huq, M. S., Loo, L.-N. D., Salter, B. J., McCollough, C. H., & Van Dyk, J. (2003). Quality assurance for computed-tomography simulators and the computed-tomography-simulation process: Report of the AAPM Radiation Therapy Committee Task Group No. 66. *Medical Physics*, *30*(10), 2762–2792. https://doi.org/10.1118/1.1609271

Verdun, F. R., Racine, D., Ott, J. G., Tapiovaara, M. J., Toroi, P., Bochud, F. O., Veldkamp, W. J. H., Schegerer, A., Bouwman, R. W., Giron, I. H., Marshall, N. W., & Edyvean, S. (2015). Image quality in CT: From physical measurements to model observers. *Physica Medica*, *31*(8), 823–843. https://doi.org/10.1016/j.ejmp.2015.08.007

Zheng, X., Al-Hayek, Y., Cummins, C., Li, X., Nardi, L., Albari, K., Evans, J., Roworth, E., & Seaton, T. (2020). Body size and tube voltage dependent corrections for Hounsfield Unit in medical X-ray computed tomography: Theory and experiments. *Scientific Reports*, *10*(1), 15696. https://doi.org/10.1038/s41598-020-72707-y